Electronic Supplementary Material (ESI) for Physical Chemistry Chemical Physics.

Molecular origin of photoluminescence of carbon dots: Aggregation induced orange-red emission

Venkatesh Gude, Ananya Das, Tanmay Chatterjee and Prasun K. Mandal*

Department of Chemical Sciences, Indian Institute of Science Education and Research (IISER) Kolkata, Mohanpur, West Bengal-741246, India.

e-mail: prasunchem@iiserkol.ac.in

Table of contents

S1: Experimental section:

Materials: Sucrose, fructose and glucose were procured from Sigma-Aldrich, H_3PO_4 was procured from Merck chemicals. For spectroscopic studies solvents like acetonitrile, and dichloromethane were procured of HPLC grade from Sigma-Aldrich. All of the chemicals were used as received without further purification.

Synthesis of CDs from Fructose and Glucose:
2g of fructose/glucose, 2mL of water and 4mL of H_3PO_4 were taken in two-neck round bottom flask and heated at 70 °C for 10 minutes. During this time the colourless solution transformed first into yellow colour then brown and then finally to black colour. After cooling the reaction mixture to ambient temperature, it was neutralized with NaOH solution. This solution was solvent extracted with dichloromethane (DCM). The dark yellow organic layer was separated. Further, excess solvent was distilled out using a rotavapour. A slurry was made using silicagel and subjected for purification using column chromatography technique with DCM as eluent. The colour of column purified CDs solution was faint brown under sunlight and when exposed to UV light of 365 nm the solution exhibit orange-red emission. Fructose, glucose derived carbon dots are abbreviated as F-CDs and G-CDs.

Characterization Techniques: FT-IR spectrum of CDs was recorded using Bruker (ALPHA) spectrometer. NMR experiments (^1H, ^{13}C and ^{31}P) were performed on Bruker Avance III 500 MHz spectrometer. XRD pattern of CDs was collected using Rigaku-smartlab diffractometer attached with CuK_α source operating at 70 mA and 35 kV. Raman spectrum was recorded using Horiba Jobin Yvon LabRam HR800 Raman spectrometer at excitation wavelength 488 nm.

Steady state and time resolved optical measurements:

(a) Steady state:

Steady state absorption and corrected emission spectra were recorded in a U-4100 Hitachi spectrophotometer and Fluoromax-3, Horiba Jobin Yvon spectrofluorimeter respectively. Solutions of all the compounds were prepared keeping in mind that the absorbance value is less than 0.1 at the absorption maxima. Φ_{Fl} (Fluorescence quantum yield) determination was accomplished by comparison of the wavelength integrated intensity of the CDs to that of the standard (Coumarin 153). Fluorescence quantum yields were calculated with solutions having absorbance less than 0.05 to avoid inner filter effect. S-CDs and the reference were excited at 425 nm. Φ_{Fl} of all the compounds was calculated using the following equation:

$$\Phi_f = \Phi_R \frac{OD_R}{OD} \frac{I}{I_R} \frac{n^2}{n_R^2}$$

Where, 'Φ', 'I' and 'n' stands for Fluorescence quantum yield, Integrated intensity and refractive index of the solvents respectively. Subscript R stands for reference.

(b) Time resolved:

Picosecond TCSPC measurement:

Fluorescence lifetime measurement at ps-ns time domain were carried out using a time correlated single photon counting (TCSPC) spectrometer (Horiba Jobin Yvon IBH). Diode laser with λ_{ex} = 281, 340, 375 and 402 nm were used as the excitation sources and an MCP photomultiplier tube (PMT) (Hamamatsu R3809U-50 series) as the detector. The width of the instrument response function (IRF), which was limited by the fwhm of the exciting pulse, was less than 100 ps for 377 nm and 402 nm excitation source. IRF was recorded using a scatterer (dilute solution of ludox in water). Nonlinear least squares iterative reconvolution procedure using IBH DAS6 (Version 2.2) was employed to fit the fluorescence decay curve using a single exponential decay equation. The quality of the fit was assessed from the $\chi 2$ values and the distribution of the residuals.

Massspectrometry: Matrix-Assisted Laser Desorption Ionization Time-of-Flight (MALDI-TOF) mass spectrometry was carried out on a Bruker ultrafleXtreme™ instrument equipped with a smart beam-II laser in the reflector mode at 22 kV acceleration voltages. 2, 5-dihydroxy benzoic acid was used as matrix.

Transmission electron microscopy (TEM): TEM images of CDs recorded using JEOL-JEM2100F at 200 kV. A small amount of CDs solution in acetonitrile drop casted on carbon coated copper grid and allowed the material for drying for 24 hours and then subjected to imaging.

Energy dispersive analysis by X-rays (EDAX): EDAX spectrum recorded using Field emission-scanning electron microscope (FE-SEM) apparatus (Jeol Scanning Microscope-JSM-6700F). A small amount of CDs solution in acetonitrile placed on a clean silicon wafer and then allowed for drying for 24 hours. The material was Au coated prior to record the spectrum.

S2: MALDI-Mass spectra of DHB matrix

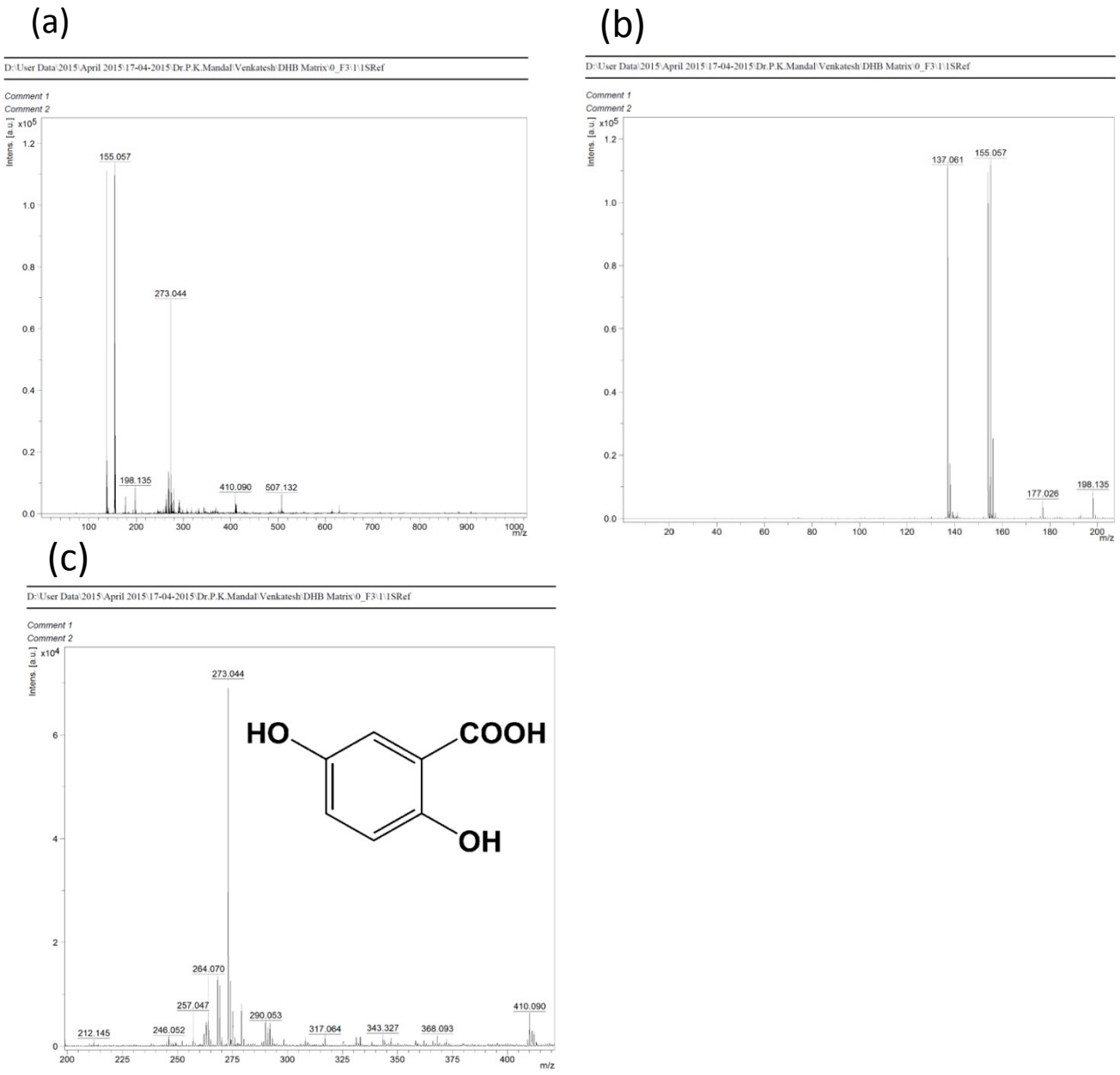

Fig. S2. Mass spectra of DHB (2,5-dihydroxy benzoic acid) matrix (a) in the region 0-1000 m/z, (b) and (c) are magnified portions of (a) in the region 0-200 and 200-450 m/z respectively.

S3: MALDI-Mass spectra of S-CDs with DHB matrix

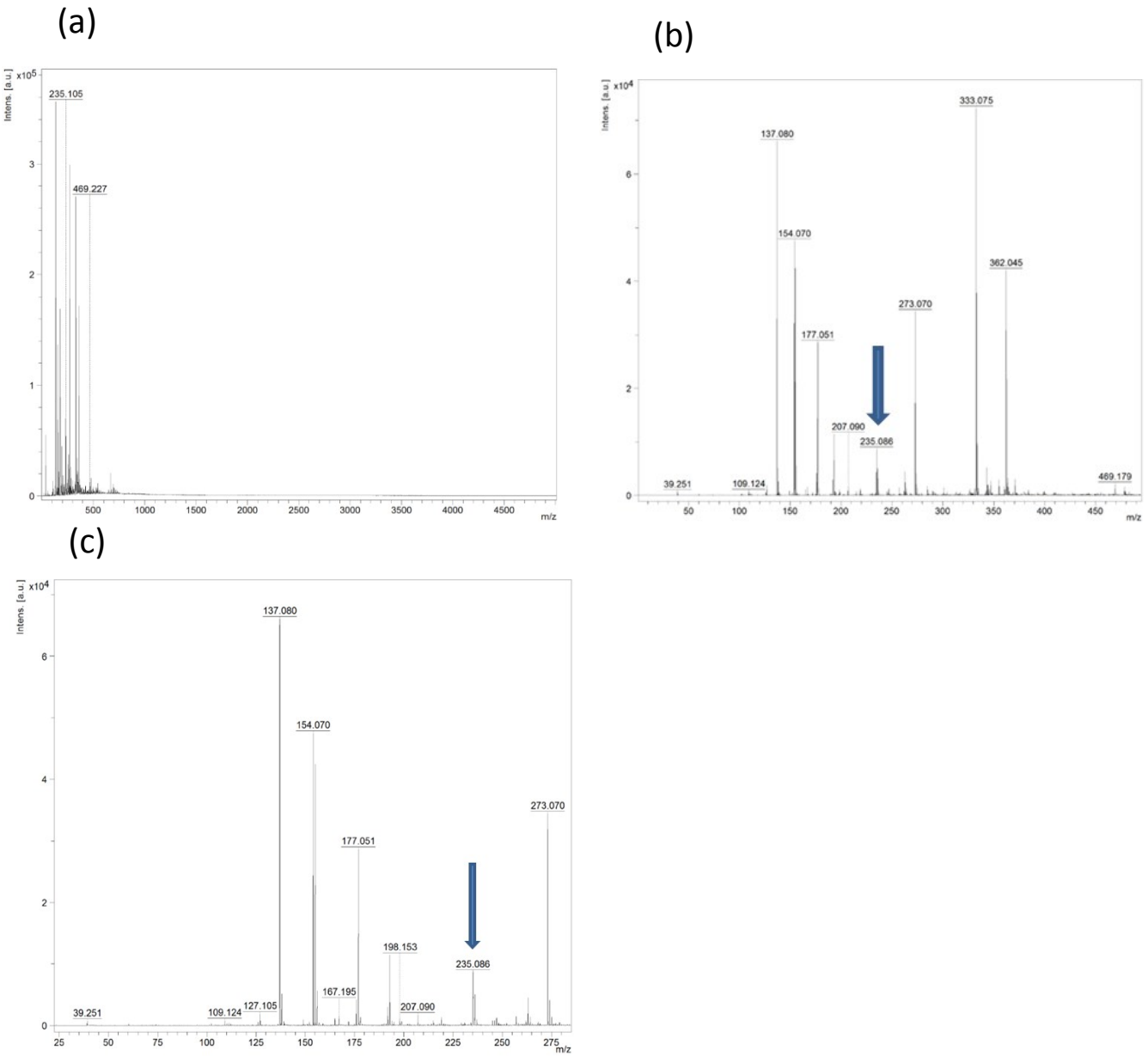

Fig. S3. Mass spectra of S-CDs with DHB matrix (a) in the region 0-5000 m/z, (b) and (c) are magnified portions of (a) in the region 0-500 and 25-280 m/z respectively.

S4: Comparison of m/z values of matrix and S-CDs

Table S1. Display of matrix (black in colour) and S-CDs (red in colour) m/z values.

Sample name	m/z values
DHB matrix	**137, 155, 177, 198, 212, 246, 257, 264, 273, 290, 317, 343, 368, 410, 507**
DHB Matrix + **S-CDs**	**39, 109, 127, 137, 154, 167, 177, 198, 207, 235, 273, 333, 362, 469**

S5: Geometry optimized structure of HMF derivative

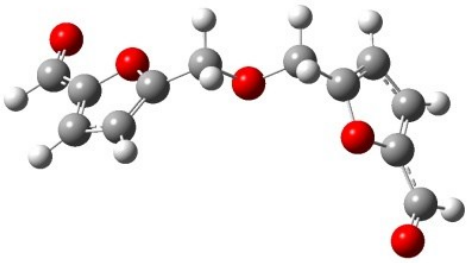

Fig. S5. Geometry optimized structure of HMF derivative of S-CDs.

The geometry of chromophore of S-CDs has been optimized by density function theory (DFT) using Gaussian 09 software.[1]All the calculations were performed using a B3LYP functional and a 6-31G basis set for all the atoms.

S6: ^{31}P NMR spectra of S-CDs

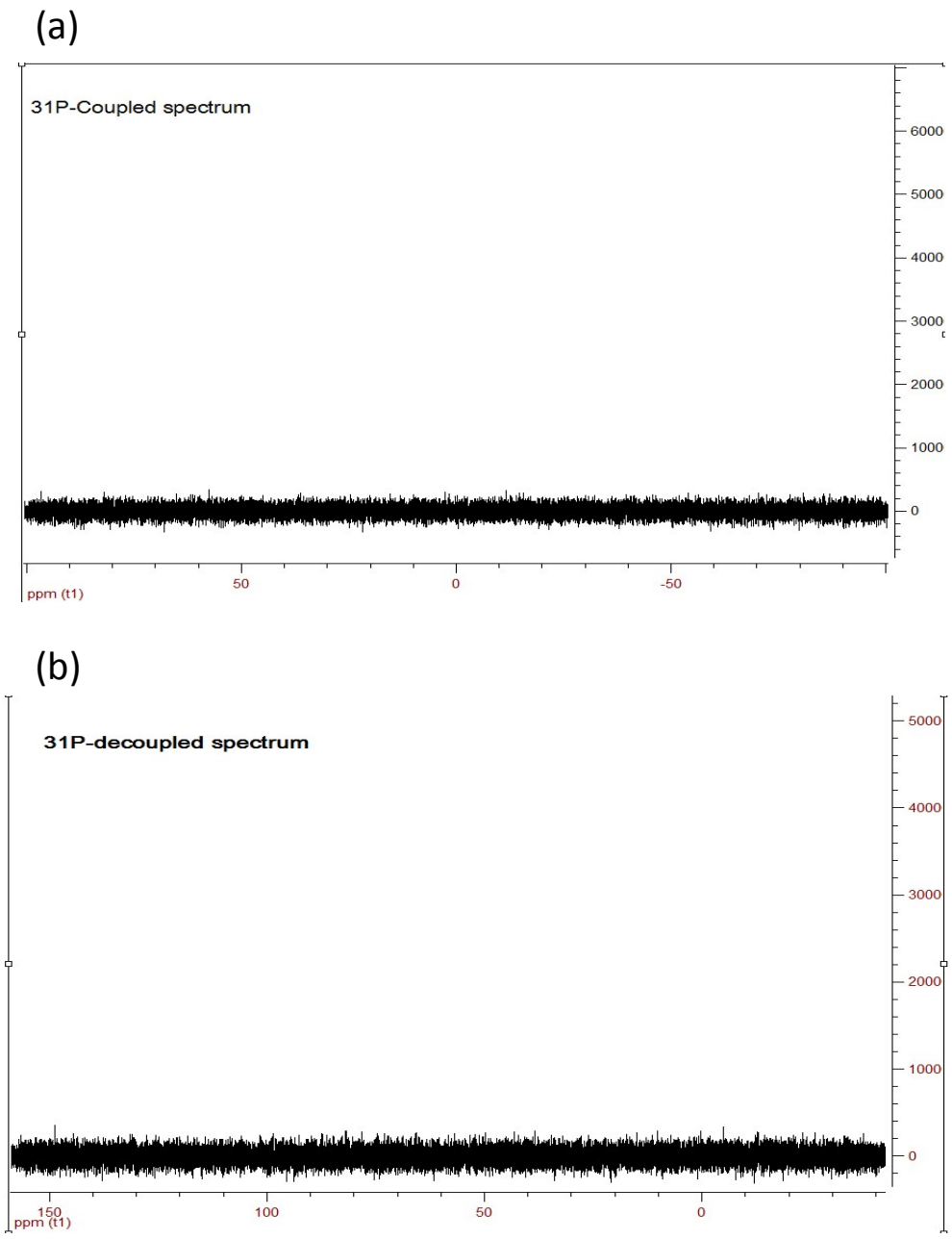

Fig. S6. (a) Coupled and (b) de-coupled ^{31}P NMR spectra of S-CDs.

S7: EDAX spectrum of S-CDs

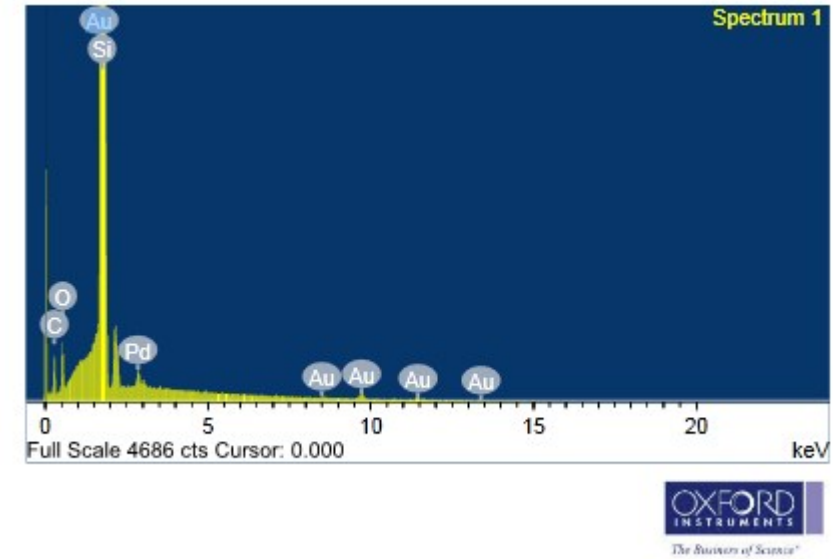

Fig. S7. EDAX spectrum of S-CDs recorded on Au coated silicon wafer.

S8: Absorption, emission and excitation spectra of furfural.

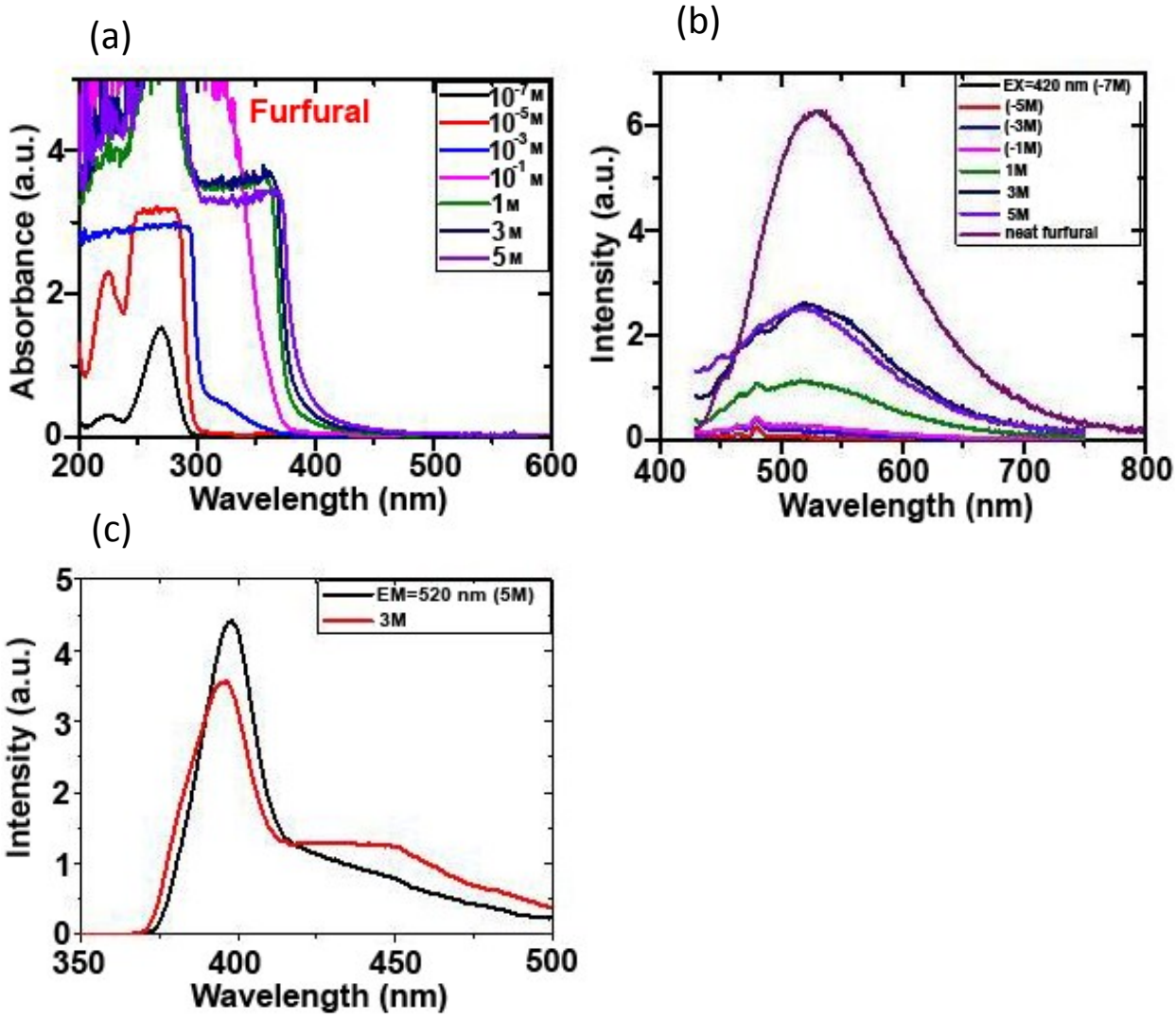

Fig. S8. (a) Absorption (b) emission at 420 nm excitation and (c) excitation spectra at monitoring wavelength of 520 nm of different concentrations of furfural in ACN.

S9: Excited state decay behaviour of S-CDs in DCM

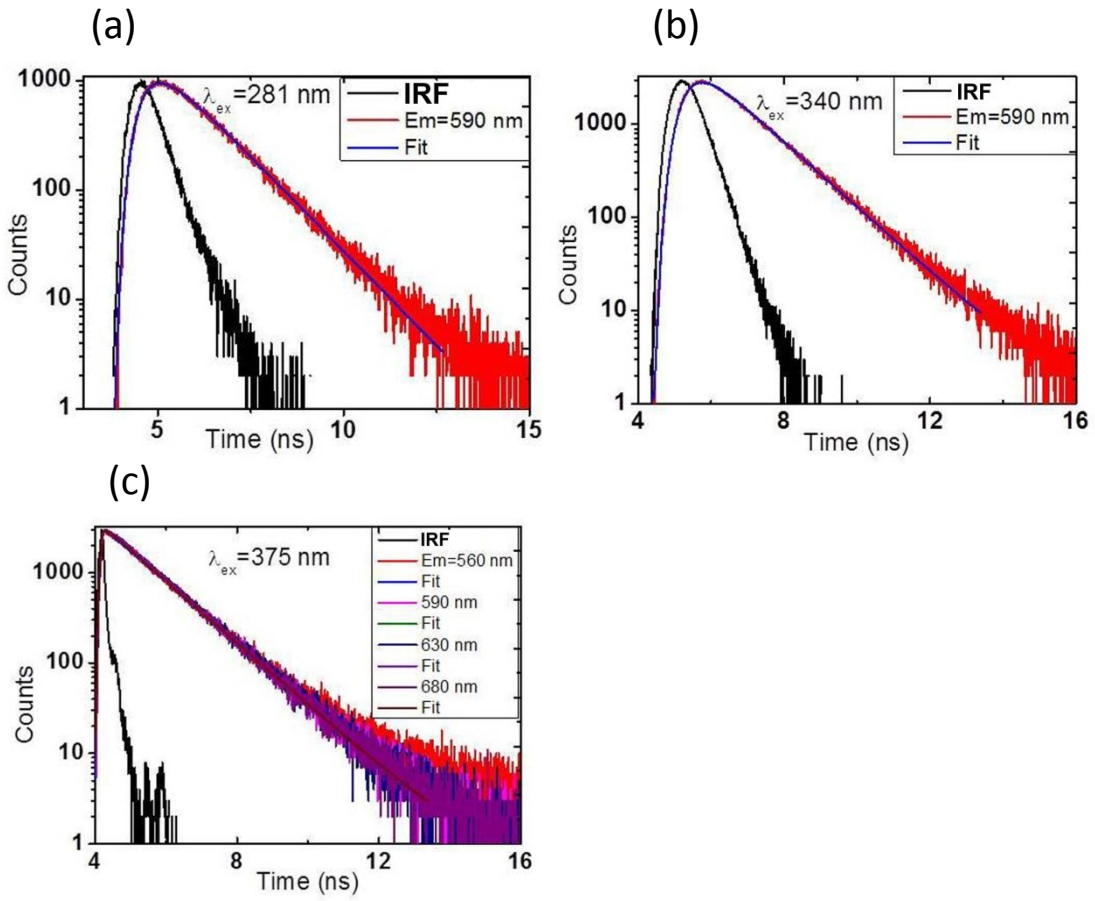

Fig. S9. PL decay curves of S-CDs in DCM at different excitation wavelengths (a) 281 nm (b) 340 nm and (c) 375 nm. Monitoring wavelengths are shown in inset.

S10: Emission, excitation and excited state decay behaviour of S-CDs in ACN

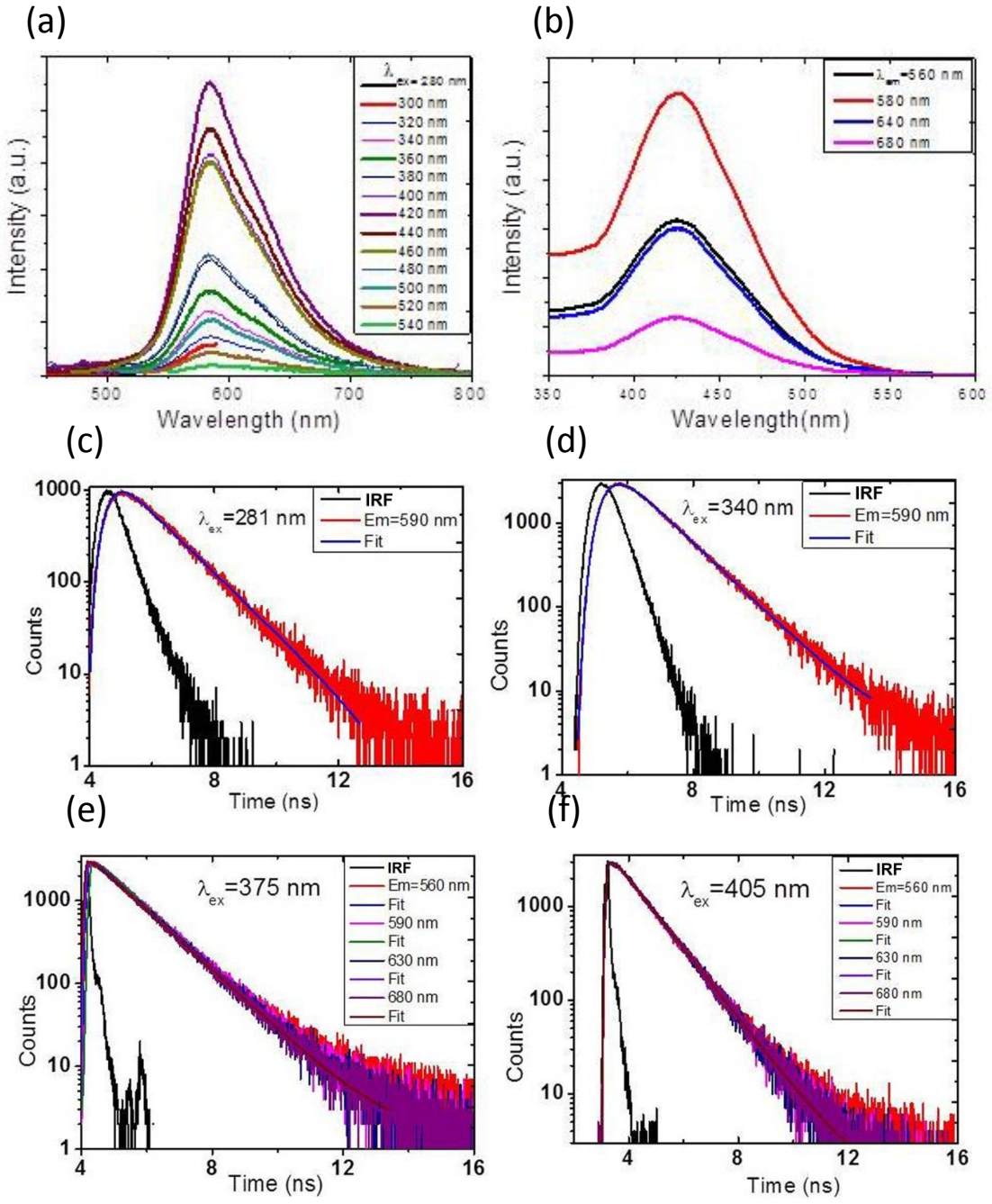

Fig. S10. (a) Emission spectra at different excitations (b) excitation spectra at different monitoring wavelengths of S-CDs. PL decay curves of S-CDs at different excitation wavelengths (c) 281 nm (d) 340 nm (e) 375 nm and (f) 405 nm in ACN. Monitoring wavelengths are shown in inset.

S11: Excitation power effect of S-CDs in ACN

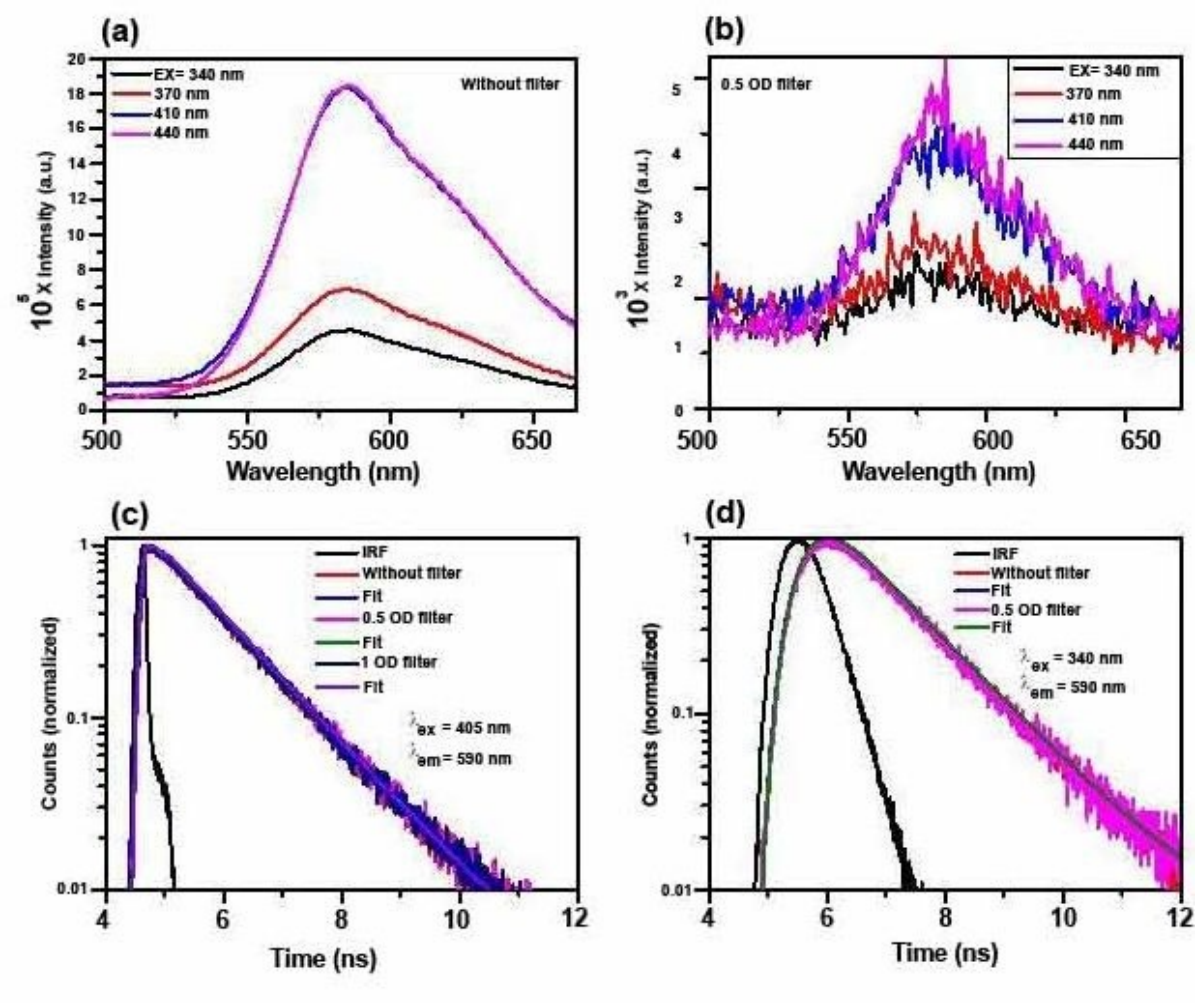

Fig. S11.Power dependent studies. PL emission at different excitation wavelengths (a) without filter and (b) with 0.5 OD filter. Comparison of PL decay traces at different excitation wavelengths (c) 405 nm and (d) 340 nm in the absence and presence of 0.5, 1 OD filter respectively.

S12: ^{1}H and ^{13}C NMR spectra of F-CDs

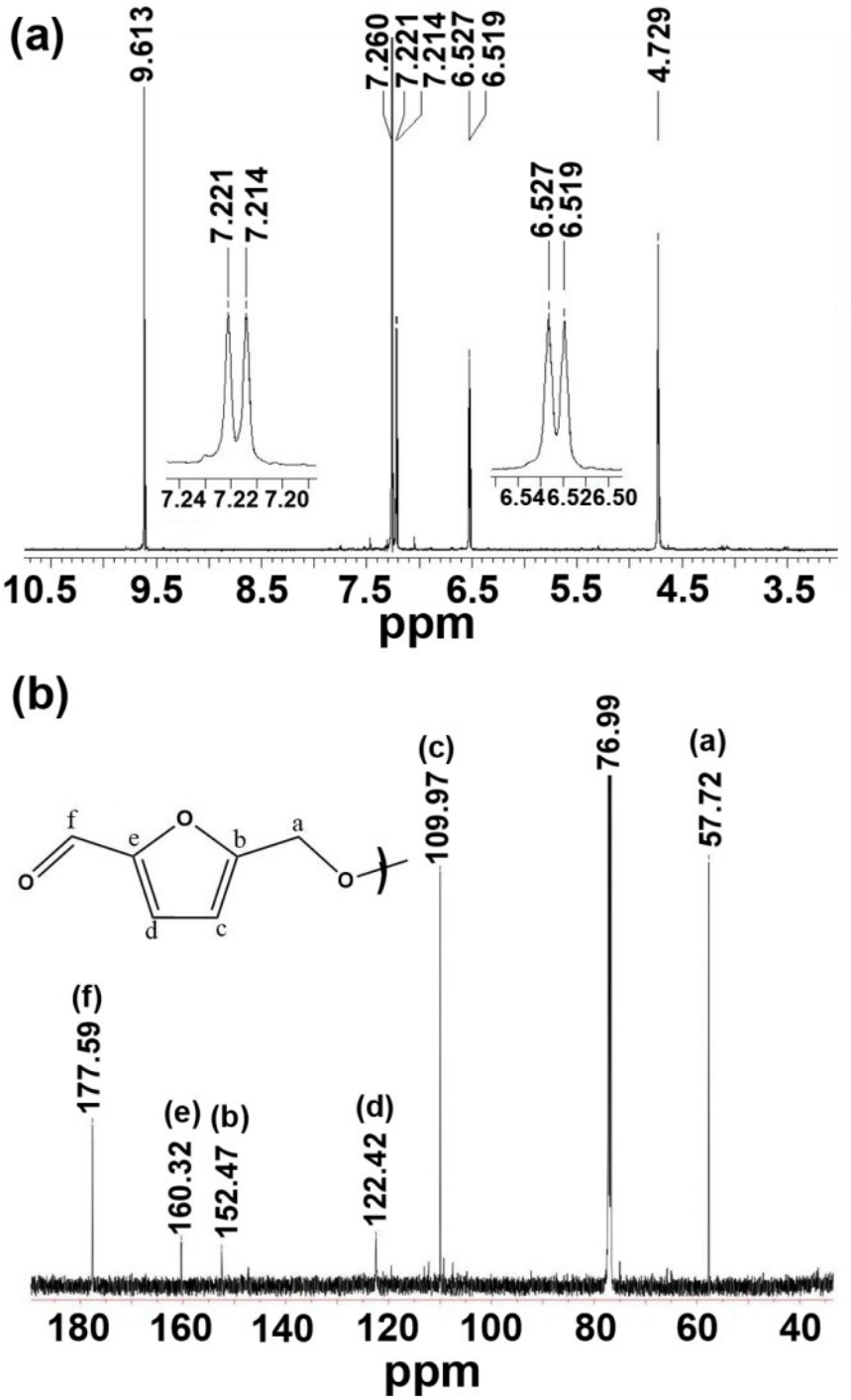

Fig. S12. (a) ^{1}H NMR and (b) ^{13}C NMR spectra of purified F-CDs in $CDCl_3$.

S13: MALDI-Mass spectra of F-CDs with DHB matrix

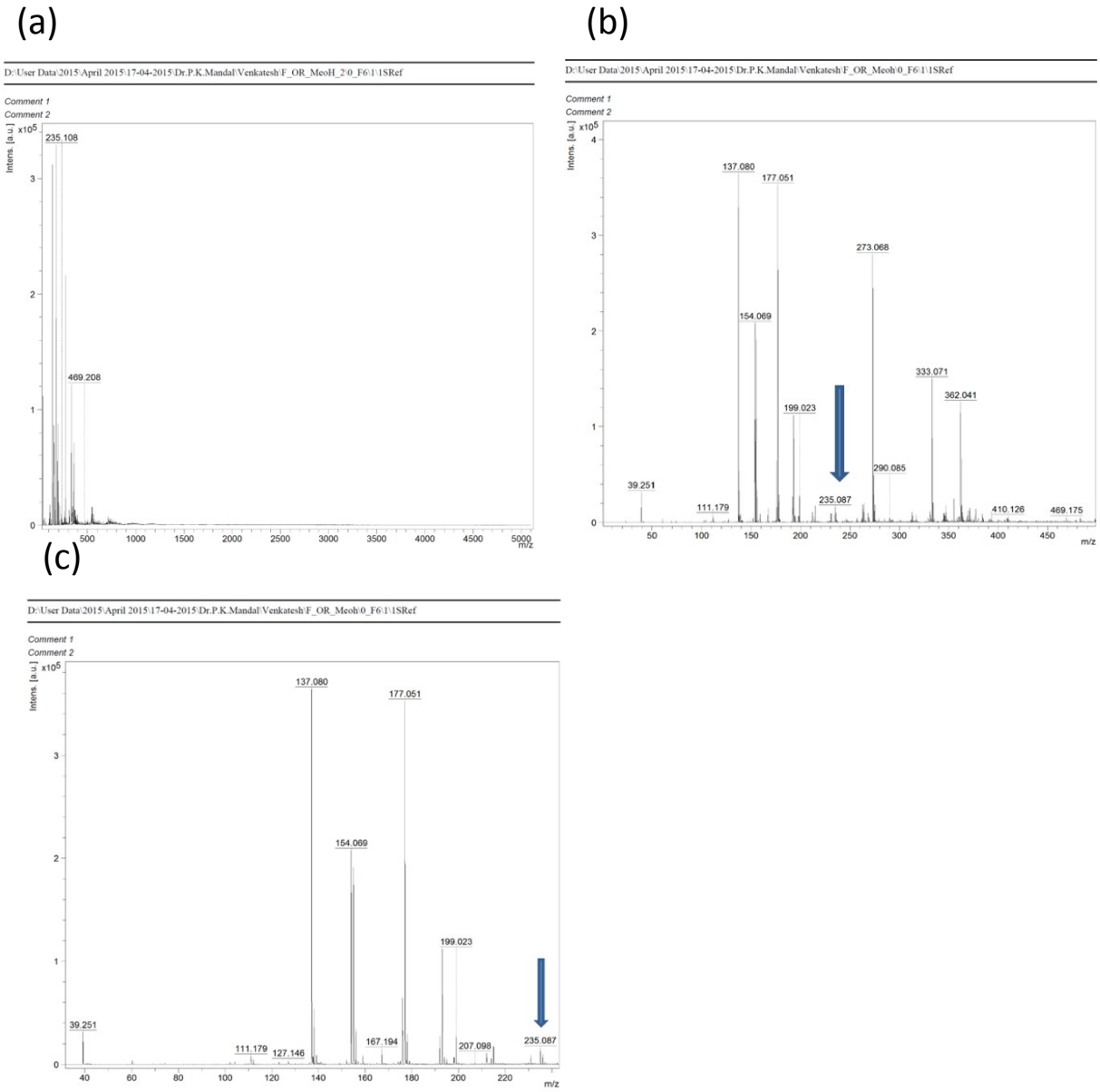

Fig. S13. Mass spectra of F-CDs with DHB matrix (a) in the region 0-5000 m/z, (b) and (c) are magnified portions of (a) in the region 0-500 and 25-250 m/z respectively.

S14: TEM image of F-CDs

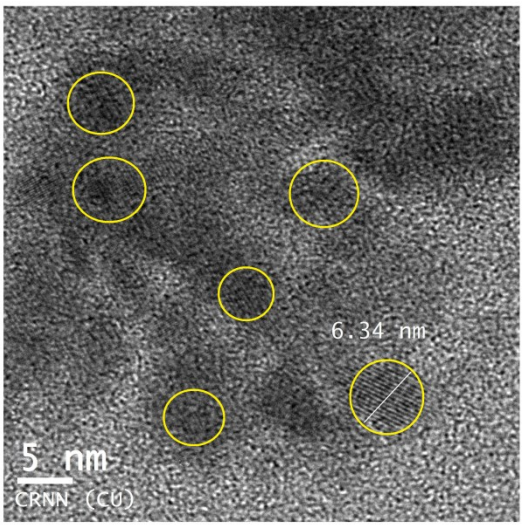

Fig. S14. TEM image of F-CDs.

S15: Emission and excitation spectra of F-CDs in ACN and DCM.

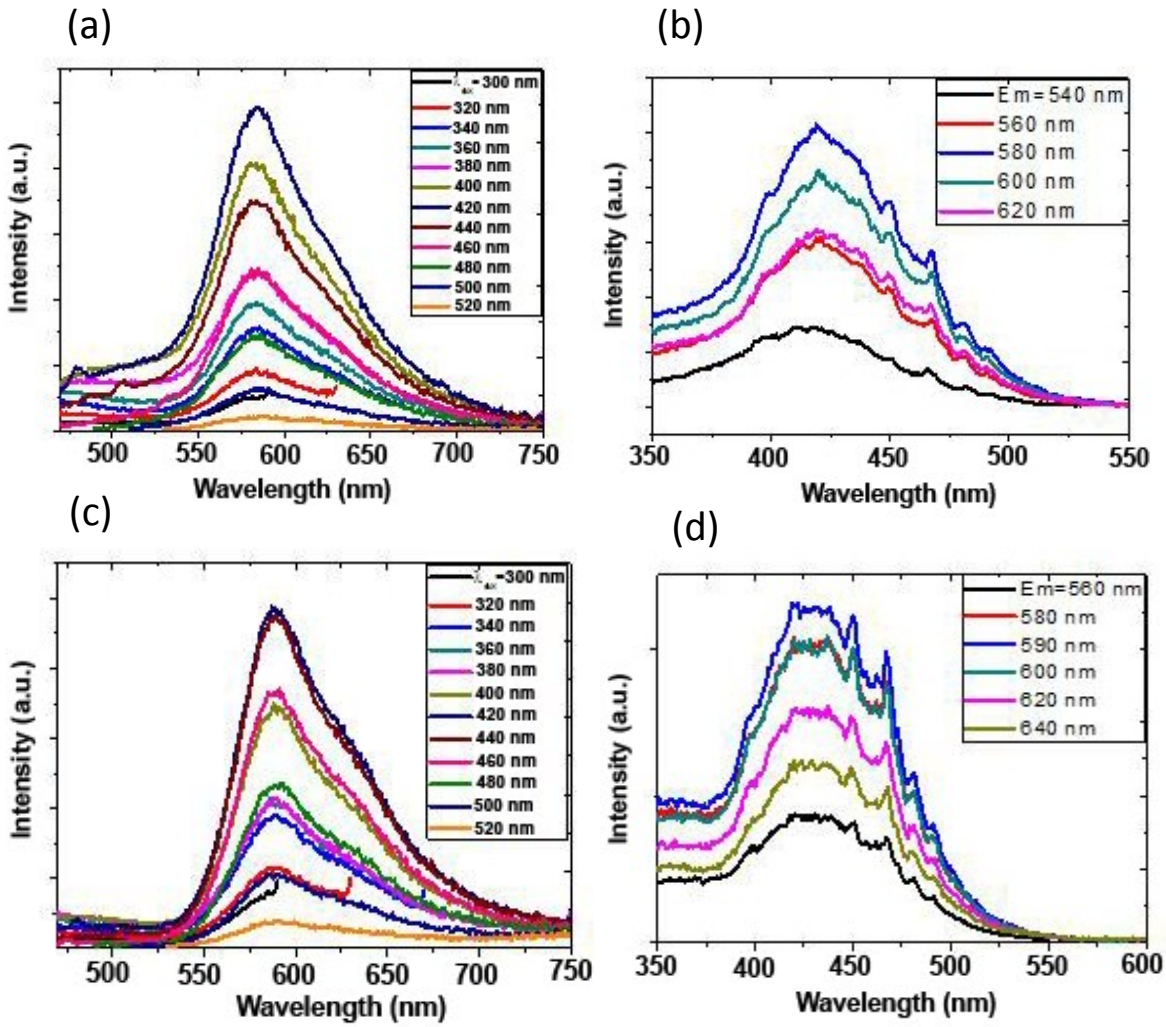

Fig. S15. (a), (c) Emission spectra at different excitation wavelengths and (b), (d) excitation spectra at different monitoring wavelengths of F-CDs in ACN and DCM.

S16: Emission and excitation spectra of G-CDs in ACN and DCM.

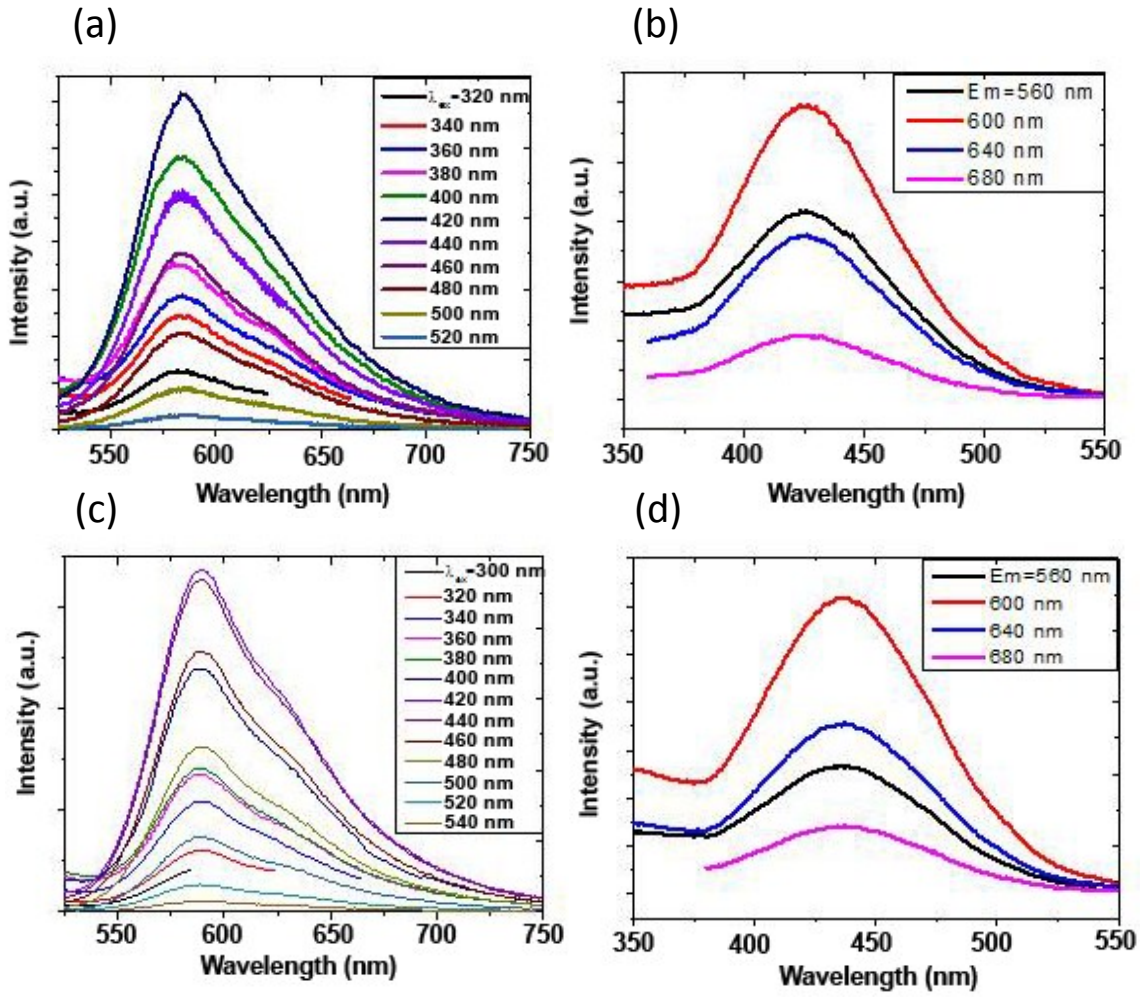

Fig. S16. (a), (c) Emission spectra at different excitation wavelengths and (b), (d) excitation spectra at different monitoring wavelengths of G-CDs in ACN and DCM.

S17: Reference:

1. Frisch, M. J.; Trucks, G. W.; Schlegel, H. B.; Scuseria, G. E.; Robb, M. A.; Cheeseman, J. R.; Scalmani, G.; Barone, V.; Mennucci, B.; Petersson, G. A.; Nakatsuji, H.; Caricato, M.; Li, X.; Hratchian, H. P.; Izmaylov, A. F.; Bloino, J.; Zheng, G.; Sonnenberg, J. L.; Hada, M.; Ehara, M.; Toyota, K.; Fukuda, R.; Hasegawa, J.; Ishida, M.; Nakajima, T.; Honda, Y.; Kitao, O.; Nakai, H.; Vreven, T.; Montgomery, J. A. Jr.; Peralta, J. E.; Ogliaro, F.; Bearpark, M.; Heyd, J. J.; Brothers, E.; Kudin, K. N.; Staroverov, V. N.; Keith, T.; Kobayashi, R.; Normand, J.; Raghavachari, K.; Rendell, A.; Burant, J. C.; Iyengar, S. S.; Tomasi, J.; Cossi, M.; Rega, N.; Millam, J. M.; Klene, M.; Knox, J. E.; Cross, J. B.;Bakken, V.; Adamo, C.; Jaramillo, J.; Gomperts, R.; Stratmann, R. E.; Yazyev, O.; Austin, A. J.; Cammi, R.; Pomelli, C.; Ochterski, J. W.; Martin, R. L.; Morokuma, K.; Zakrzewski, V. G.; Voth, G. A.; Salvador, P.; Dannenberg, J. J.; Dapprich, S.; Daniels, A. D.; Farkas, O.; Foresman, J. B.; Ortiz, J. V.; Cioslowski, J.; and Fox, D. J. Gaussian, Inc., Wallingford CT, **2010**